Site Specific Propagation Model Development

Chriss Hammerschmidt, Robert T. Johnk
Institute for Telecommunication Sciences
NTIA
Boulder, CO, USA
chammerschmidt@ntia.gov

***Abstract*— Propagation models are used to inform scientists and engineers on how radio propagation through an environment will affect the radio signal received on the other end of the link. Many propagation models have been developed: some are curve-fitting models, some are based on the physics of the propagation path. Some models have been developed that incorporate the presence of vegetation and man-made structures (clutter) to more closely approximate measured data. However, no model thus far predicts path loss in all environments (urban, suburban, rural, forested, etc.). This paper introduces various propagation models and compares them to measured data. In the end, we present another predictive model that includes objects within the first Fresnel zone as a predictor for a more inclusive propagation model.**

***Keywords*—clutter, Fresnel zone, measurements, mobile propagation, propagation models**

I. Introduction

Wireless communication depends on the transmission frequency, the transmitted power, the heights and gains of the transmitting and receiving antennas, the distance the wave travels, and any intervening vegetation, terrain, or man-made structures between the transmitting antenna and the receiving antenna. Communication systems are often designed based on measurements performed in the area where the system will be deployed. When only a few transmitters and receivers are deployed and they are stationary, then simple models can be developed to understand how the radio signals travel between the various transmitters and receivers. As new communication systems, such as cellular systems, were developed over the years, many measurements were made to better understand the radio propagation environment and create a better radio propagation model.

The most widely used propagation model is a linear fit to propagation data. The standard deviation is used to explain the signal variability. One complication to using this type of model is that the paths from transmitting antenna to receiving antenna do not typically traverse homogeneous environments. Another complication to model development is that urban areas and towns are often redeveloped, modernized, and drastically modified so previous measurement data may no longer be valid.

Over the past 20 years or so, information from terrain databases and documentation about buildings and trees have become better, more accurate, and ubiquitous. The current propagation modeler has access to vast resources and computing power. All of this information is available to create newer and more realistic models.

The goal of this paper is to familiarize the reader with some current models and compare them to recently measured data. We discuss why the current model may not compare well to the measured data and discuss how the model could be improved with more information from the propagation environment.

II. Propagation Model vs. Measurement

Radio propagation between a transmitting antenna and a receiving antenna is governed by the Friis transmission equation,

$$P_r = \frac{P_t G_t G_r \lambda^2}{(4\pi)^2 d^2 L} \tag{1}$$

where P_r is the received power in watts, P_t is the transmitted power in watts, G_t and G_r are the gains of the transmitting and receiving antennas, λ is the wavelength of the transmitted signal in meters, d is the distance between the transmitting and receiving antennas in meters, and L is any additional system losses. This formula tells us the major contributors to the propagation of any RF signal. This formula is used to develop propagation models from a very simple model such as the free-space transmission loss (FSTL) formula, to more extensive models that include losses from terrain, vegetation, and man-made structures.

A. Free-space transmission loss (FSTL)

The FSTL is calculated from (1) using the following formula:

$$FSTL = \frac{(4\pi d)^2}{\lambda^2}, \tag{2}$$

rearranging terms and putting FSTL in decibels (dB),

$$FSTL = 32.4 + 20\log_{10} f_{MHz} + 20\log_{10} d_{km} \tag{3}$$

where f_{MHz} is the transmission frequency in MHz and d_{km} is the distance between antennas in km. In this paper, plots are shown in terms of basic transmission gain (BTG) or free-space transmission gain (FSTG) which are both defined as the inverse of basic transmission loss (BTL) or FSTL.

Fig. 1 shows measured BTG vs. the FSTG. The measured BTG is shown by the black x's and the FSTG is shown by the blue line. The measured data was taken from a transmitting location in a parking lot to a receiving location on a street at a distance of 230 meters in downtown Phoenix, AZ. The receiving antenna was stationary and there were no intervening objects, so the variability in the measured data is due to movement of surrounding scattering objects such as cars. The ground was relatively flat along this path.

This paper was presented at, and appears in the proceedings of, the 2019 IEEE International Symposium on Electromagnetic Compatibility, Signal & Power Integrity (EMC+SIPI). IEEE

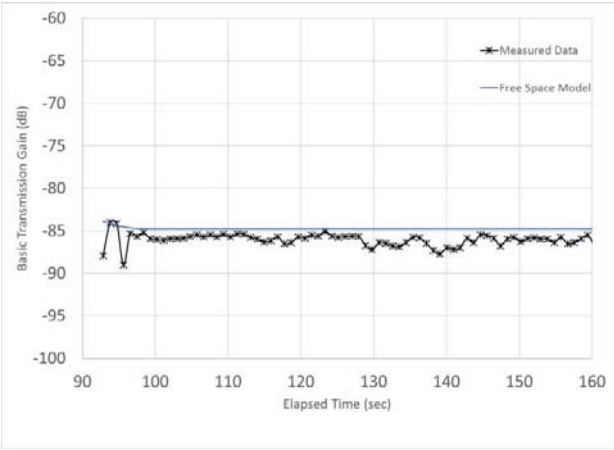

Fig. 1. Measured BTG and free-space transmission gain (FSTG) in dB for a stationary receiving antenna.

To analyze the area in greater depth, Google Earth™ has the capability to do a viewshed analysis [5], [6]. Viewshed analyses show us receiving locations that are line-of-sight (LOS) (no obstructions) to the transmitting antenna. In Fig. 2, the transmitting antenna is at the North Lot pin and the receiving antenna from Fig. 1 is at the pushpin shown in the upper left of the figure. The green areas show the analysis for areas with a LOS view to the transmitting antenna at a height of 18.2 m for a receiving antenna at a height of 3 m. The buildings and other cars on the road are what contribute to the measured signal variability. The FSTG is a pretty good model for this stationary, LOS receiving antenna.

B. Log-Distance path loss model

This model uses a linear-least square fit to the data when the ordinate data is in units of log-distance. The equation used for the fit is

$$L(dB) = FSTL(d_0) + 10n\log_{10}\left({}^{d}/_{d_0}\right) + \mathrm{X}_{\sigma} \qquad (4)$$

where d_0 is a reference distance, n is the exponent used to describe the loss, d is the distance in km between the transmitting and receiving antennas, and X_σ is the distribution that describes the shadow fading in the data [1]. Fig. 3 shows a plot of measured basic transmission gain (black x's) taken in a densely forested suburban area near Chapel Hill, North Carolina. Also included on this plot is the log-distance fit to the data (red line). The standard deviation is calculated to estimate the signal variability (magenta lines) [2]. In the data, our eyes can pick out two distinct data slopes which are not reflected in this model. Also, the standard deviation does not completely explain the variability in the data; at some locations there is more variability, in other locations there is less.

In the actual measurement, we encountered terrain, vegetation, and man-made structures. The trees in this area of North Carolina can be between 15 m and 22 m (50 and 70 feet) tall and can surround the receiving antenna as shown in Fig. 4. We see that the ground rises at the end of the street and that the trees form a canopy over the receiving antenna on top of the van. This picture can explain the difference between the model and the real measurement and tells us that we include effects from terrain, trees, and man-made structures.

C. Longley-Rice, Irregular Terrain Model (ITM)

As the propagation path becomes longer and includes hills and mountains, we need to have a model that includes terrain attenuation. The Irregular Terrain Model (ITM) was developed to address terrain and variability in measured data. ITM was developed at the Institute for Telecommunication Sciences (ITS) in the 1960s [7], [8].

To understand the ITM model, we have taken a measurement with a stationary transmitting antenna and a receiving antenna in motion at the Table Mountain Research facility just north of Boulder [9]. This is a very flat mesa, with little vegetation and only a few man-made structures. Fig. 5 shows the drive route on top of Table Mountain. The transmitting antenna is shown by the yellow cross, the red dots show the drive route for the receiving antenna, and the edge of the mesa is shown by the horizontal yellow line.

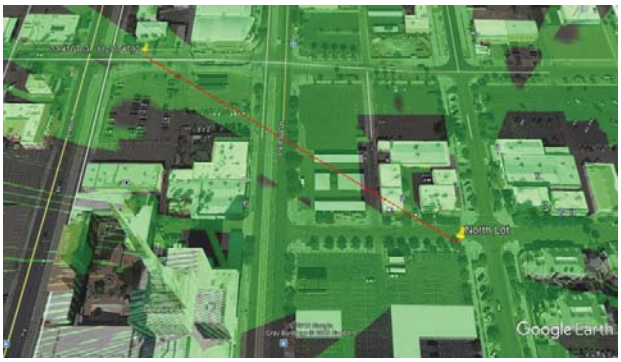

Fig. 2. Viewshed Analysis results. The transmitting antenna was at the North Lot position and the receiving antenna is shown at the upper left corner. Green corresponds to line-of-sight regions.

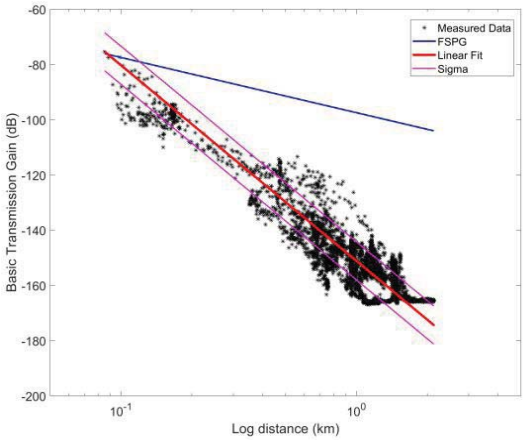

Fig. 3. Log-distance linear fit (red line) plus sigma (magenta lines), measured data (black x's) in Chapel Hill, North Carolina. Free-space transmission gain is shown by the blue line.

This paper was presented at, and appears in the proceedings of, the 2019 IEEE International Symposium on Electromagnetic Compatibility, Signal & Power Integrity (EMC+SIPI). IEEE

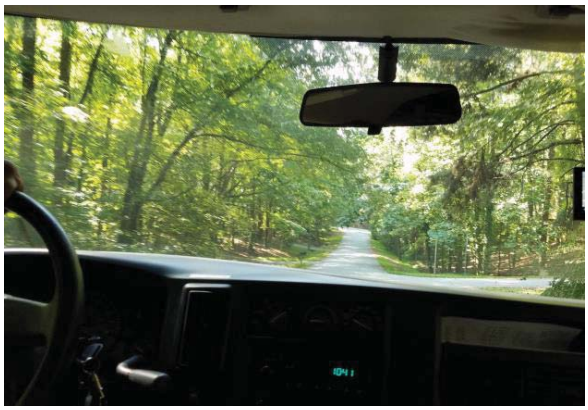

Fig. 4. Receiving van making a measurement in a suburban, forested area of Chapel Hill, NC.

Fig. 6 shows the measured and modeled results. The measured BTG is shown by the black x's, the FSTG is shown by the blue line, and the red diamonds show the results from ITM. From 375 s to approximately 395 s and from approximately 450 s to 475 s, the receiving van was on the top of the mesa and then from 395 s to 450 s the receiving van drives over the edge of the mesa to a lower plateau and then returns over the ridge to the top of the mesa. The FSTG model (blue trace) does not include the terrain ridge encountered by the RF signal and so it does not predict attenuation due to this ridge. However, when we use ITM, which uses a terrain database and models diffraction from the ridge, the attenuation to the radio signal due to this terrain feature is accurately predicted. Again, the variability in the measured data is due to multipath scatterers in the vicinity of the receiving or transmitting antenna. ITM calculates channel variability shown by the yellow and green traces in Fig. 6. ITM is a very good model for terrain attenuation; however, the results do depend on accuracy of the underlying terrain database [10].

D. Okumura-Hata model

Yoshihisa Okumura measured average field strength at four different frequencies from 400 MHz to 2000 MHz in the 1960s in the Kanto region in Tokyo, Japan [11]. The data was taken for transmitting antenna heights in m for frequencies from 30 to 1000 MHz and for distances from 1 to 100 km. The

Fig. 5. Table Mountain map showing mobile drive route (red circles), the transmitting location (yellow cross), and the edge of the mesa (yellow horizontal line).

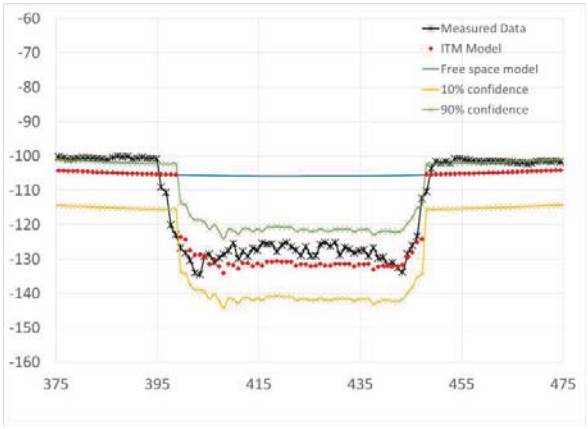

Fig. 6. Measured BTG, FSTG, and ITM model for a mobile receiving antenna on Table Mountain.

receiving antenna was placed on a mobile van and its height above ground was 3 m. Paths were selected in areas with hilly and mountainous terrain, built-up cities, and in quasi-smooth areas. Curves were fit to the data to provide insight into land-mobile propagation in urban and terrain obstructed areas.

In the 1980's, Masaharu Hata [12] derived empirical formulas from Okumura's report to aid in computing generalized formulas to predict propagation in what he termed urban, suburban, and open areas. The dependent variables for these models are frequency, transmitting and receiving antenna heights, and distance. Intrinsic to these formulas is the dependence on terrain, buildings, and foliage measured between the two antennas. Fig. 7 shows the same measured data as Fig. 3, along with the FSTG model, and the Hata empirical formulas for the open and suburban areas. We notice that the model trend is pretty good for distances less than 0.5 km. The slope changes at this point due to the propagation through trees. Also, the Okumura-Hata model was developed for transmitting antenna heights >30m and our transmitting antenna was at 20 m. The model was also generated for distances >1 km, so the model does not exactly fit our measured data parameters. Another explanation is that this model may not fit our data because we are in a heavily forested area, so let's try to fit the model to an urban/suburban location.

The data shown in Fig. 8 is for the urban/suburban areas of Los Angeles, CA. The urban model should fit the data since Los Angeles would likely be more similar to the Tokyo data than would the heavily forested suburban areas in North Carolina. We have plotted the four different Okumura-Hata models plus FSTG. We see that slopes for these models do not fit the slope of the measured data in the Los Angeles area. In fact, from approximately 1.8 km to 2.8 km, the slope is opposite to what is normally seen in these types of plots. Is this data bad or is there an explanation? Let's probe a little further into the measured data.

Fig. 9 shows the same measured data as Fig. 8 but the measured data is now coded according to whether the area could be classified as suburban, urban, or dense urban. Fig. 10 shows the colored streets plotted on a visual map. The dark blue color is an area known as Elysian Park which has some

This paper was presented at, and appears in the proceedings of, the 2019 IEEE International Symposium on Electromagnetic Compatibility, Signal & Power Integrity (EMC+SIPI). IEEE

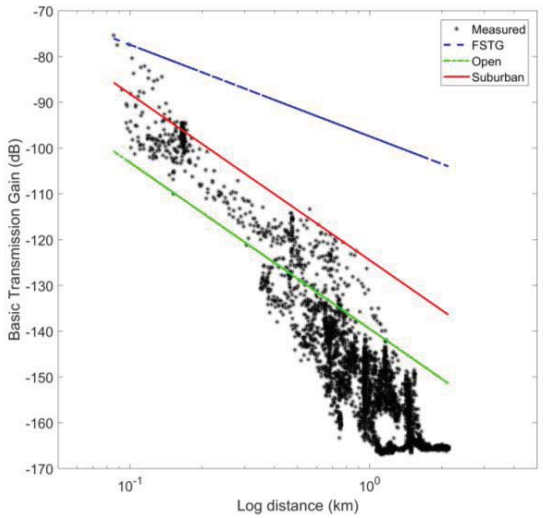

Fig.7. Measured data (black *), FSTG (blue line), and two Okumura-Hata models for suburban (red line) and open (green line) areas fit to propagation data taken in Chapel Hill, NC.

housing but is mostly park and is surrounded by suburban Los Angeles. The orange color indicates a suburban/small urban area around Chinatown just outside the downtown area. The red color indicates an area on the eastern side of downtown Los Angeles which is urban industrial, as is the area shown by the yellow color on the south side of downtown. The light blue area shows measurements in the dense urban area of downtown Los Angeles, and the green circles are a street in the downtown area of Los Angeles with the start of the run down Dewap St. shown by the dark blue asterisk and the end of the run shown by the maroon asterisk. The ITM model along Dewap St. is shown by the open olive circles and the free-space model is shown by the magenta triangles.

As we said before, ITM predicts attenuation due to terrain

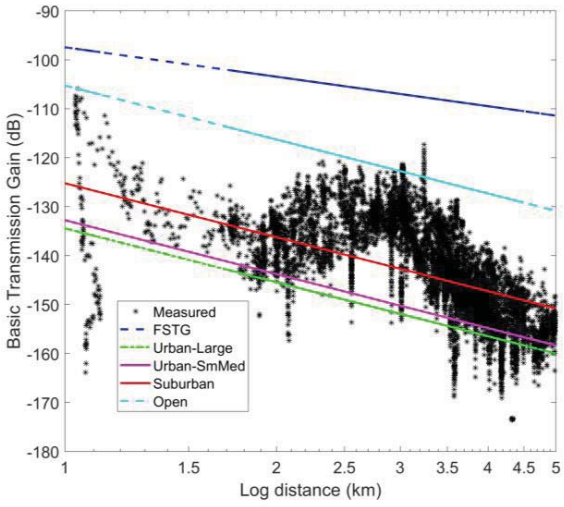

Fig. 8. Measured data (black *), FSTG (blue line), and two Okumura-Hata models for suburban (red line) and open (green line) areas fit to propagation data taken in Los Angeles, CA.

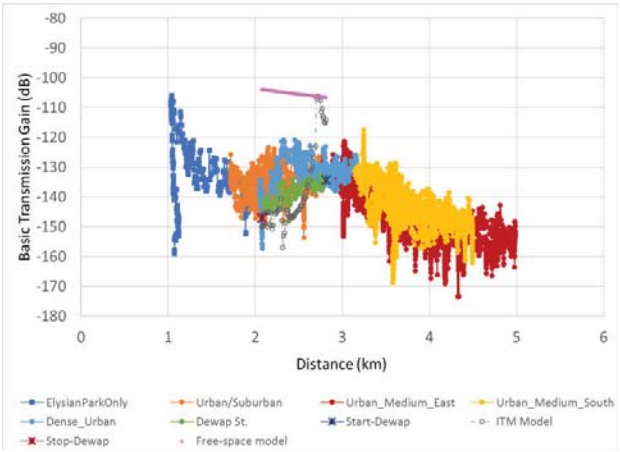

Fig.9. Measured data showing data points by color in suburban, urban, and dense urban areas of downtown Los Angeles, CA. Included in the plot are the ITM model (open circles) and free-space model (magenta triangles) for Dewap St.(green circles) in the dense urban area.

obstructions plus variability. There is a large hill between the transmitter and receiver for the closer distances on Dewap St. so that would explain the lower transmission gain at close distances. We also see that ITM predicts no terrain interaction around 2.8 km so there is no terrain attenuation (ITM equals FSTG). A small hill exists for distances from about 2.8 km to 2.9 km so ITM predicts a small amount of terrain attenuation.

As we look at the different models and their comparison to the measured data, we still see a difference between ITM and the measured results. We attribute this to the vegetation or manmade structures which we call “clutter” [13]. If one were to look at this on Google Earth, one would see that numerous trees and buildings intersect the propagation path which tells us is that we need a propagation model that is path specific to include the effects of the objects in the path.

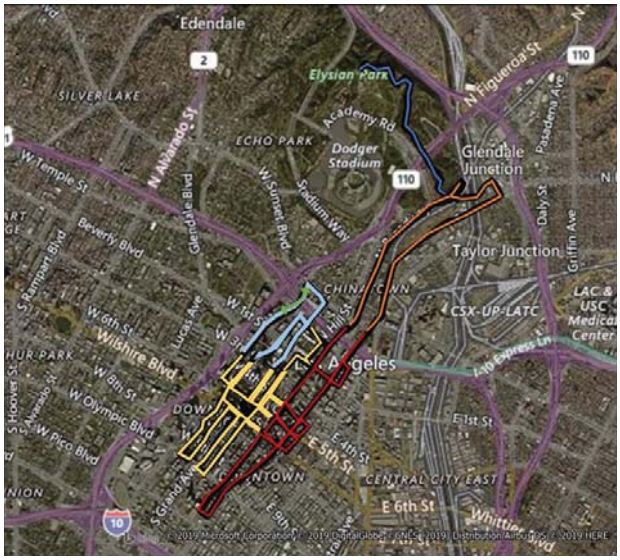

Fig.10. Colored measurement routes in downtown Los Angeles corresponding to those shown in Fig. 9.

This paper was presented at, and appears in the proceedings of, the 2019 IEEE International Symposium on Electromagnetic Compatibility, Signal & Power Integrity (EMC+SIPI). IEEE

E. Newer models

We have learned in the last few sections that distance, terrain, foliage, and man-made structures are important to propagation models. Some of the ways we can get this information are from terrain databases, land-cover databases, shape files, and Light Detection and Ranging (LIDAR) databases. Terrain databases include "The National Map" maintained by the United States Geological Services (USGS) and Digital Terrain Elevation Databases (DTED), two of the most widely used. Land-cover databases can be obtained from both the USGS website and "LandFire" database [14]. Shape files can be obtained from some government entities such as municipalities and from GIS software programs like ESRI ArcGIS [15] or QGIS [16]. LIDAR databases contain information on terrain, foliage, and buildings. Although these types of databases do not contain information on all the United States, they are quickly becoming a national resource. The Army Corps of Engineers is one of the leaders in providing this type of information.

ITS has been developing and looking into several different models to understand propagation on a path-by-path basis in recent years. The first such effort was an extension to the Okumura-Hata propagation model [17]. The urban model incorporates ITM, curve fit extensions to 3.5 GHz from the Hata formulas, and information from the National Land-Cover Database (NLCD). The NLCD database contains categories of land cover such as urban, forests, and farmlands [18]. In the second model under development at ITS, the NLCD is used along with measured data to fit land-use classification categories to different types of clutter distributions and train a model that could be used to explain propagation in different areas of the United States. The main categories currently used are Dense Urban, Urban, Suburban, Suburban Forested, Rural, Rural Forested, and Barren. This model is still be refined but is expected to be published in an IEEE Journal in the coming year.

In 2015, ITS was working with the National Institute of Standards and Technology (NIST) on a different formulation for a propagation model. We used measured data from a suburban area of Boulder, Colorado, called Martin Acres. The transmitting antenna was located on a mesa behind the Department of Commerce (DOC) Boulder Laboratories [19]. A graph of this data is shown in Fig. 11. The measured data (blue x's) from approximately 300 s to 1400 s is the data in the Martin Acres neighborhood from a transmitting antenna on the mesa. The ITM model predictions are shown by the red asterisks, and FSTG is shown by the black line.

We decided to use ITM's knife-edge diffraction model on LIDAR data to predict attenuation. LIDAR includes building and tree information for each path profile. A 3D view of LIDAR data in this neighborhood is shown in Fig. 12. We can see the outline of trees and buildings. We chose four streets from the measured data in this neighborhood and ran ITM using the LIDAR data. One of the profiles ingested by ITM is shown in Fig. 13. The blue trace is the terrain profile including terrain obstructions, foliage, and man-made structures. The transmitting antenna is at 0 km on top of the mesa and the receiving antenna is located at the farthest distance. The direct

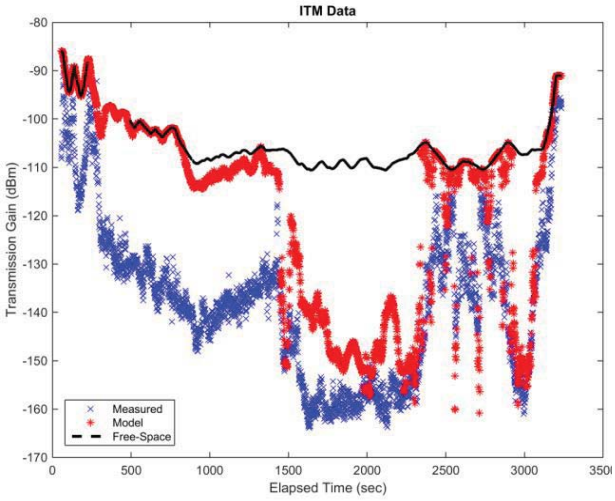

Fig.11. Measured data in the Martin Acres neighborhood near the DOC Boulder Laboratories.

LOS path is shown by the red trace from antenna to antenna, and the green traces show the extent of the first Fresnel zone. We see that the first Fresnel zone is intersected by two objects from the LIDAR dataset. When we ingested the blue profile into ITM we obtained no meaningful attenuation values from ITM so we refined our model. We incorporated a linear regression model using several different predictors.

Fig. 14 shows the results from our linear regression models. This data was taken along Lashley Lane in Martin Acres. The measured data is shown by the black circles. The first prediction using ITM on LIDAR data (ITM+LIDAR) to predict propagation losses is shown by the red asterisks. Most of the ITM+LIDAR predictions are uninformative. If distance is used as a predictor (blue line), the model gets us in the ball park, but no fine detail like that shown in the measured data is available. If we use predictions from both ITM+LIDAR and distance, the prediction gives us better agreement with the measured data as shown by the red trace. As a final model, we consider the

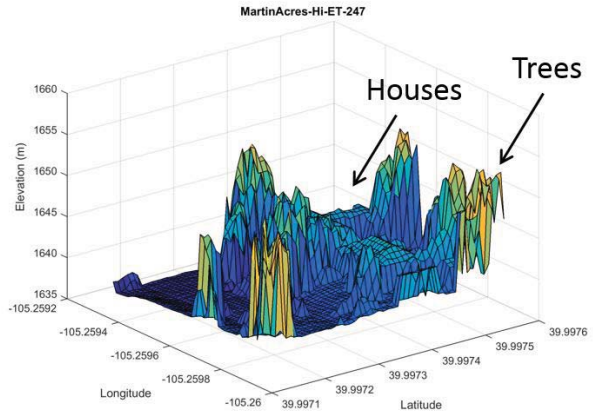

Fig. 12. LIDAR data for an area in Martin Acres. Horizontal resolution is 1 m.

This paper was presented at, and appears in the proceedings of, the 2019 IEEE International Symposium on Electromagnetic Compatibility, Signal & Power Integrity (EMC+SIPI). IEEE

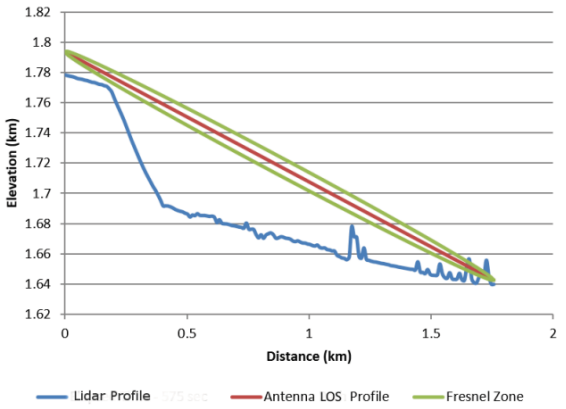

Fig. 13. LIDAR profile (blue trace), LOS direct path (red trace), and first Fresnel zone (green trace) for a path in Martin Acres.

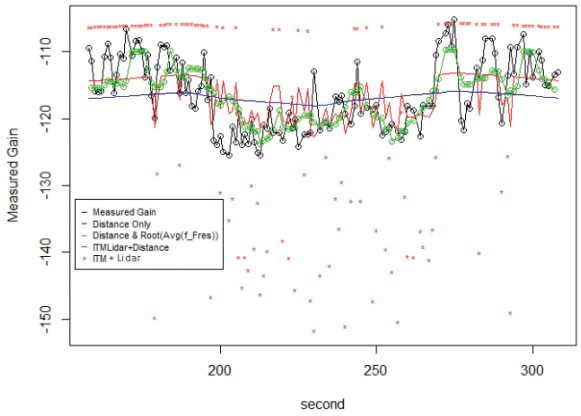

Fig.14. Different predictions for various propagation model linear least-square models.

objects in the profile that cross into the Fresnel zone and take an average of the predicted losses of the four locations surrounding the current location. This gives us an even better prediction of the measured data for these paths as shown by the green circles. We began this model over four years ago and have not had a chance to apply it to other datasets yet. Over the next year we plan to research the efficacy of this model on various measured datasets where we can use LIDAR information to obtain propagation losses.

III. Conclusion

We have introduced various models that use frequency, distance, terrain features, vegetation or foliage, and building profiles as propagation loss predictors. We have shown that frequency and distance get us in the ballpark of our measured data. Terrain attenuation adds more value as a predictor, but we have found that we need to include losses associated with man-made structures and foliage to get a more accurate propagation model.

Acknowledgment

We thank Eric Nelson, Group Leader at ITS, and the Defense Spectrum Office for funding to support measurements.

References

[1] T. K. Sarkar, Z. Ji, K. Kim, A. Medouri, M. Salazar-Palma, "A Survey of Various Propagation Models for Mobile Communication," IEEE Anten. and Propag. Mag., Vol. 45, No. 3, June 2003.

[2] J. Andrusenko, J. Burbank, J. Ward, "Modeling and Simulation for RF Propagation," Design & Developers Forum IEEE Globecom 2009, December 2009.

[3] R. T. Johnk, C. A. Hammerschmidt, I. Stange, "A High-Performance CW Mobile Channel Sounder," Proc. 2017 IEEE Int. Symp. Electromag. Compat. & Sig. Power Integ. (EMSCI), Washington D.C., August 2017.

[4] R. T. Johnk, C. A. Hammerschmidt, M. A. McFarland, J. J. Lemmon, 'A fast-fading mobile channel measurement system,' IEEE Conf. Electromag. Compat. 2012, pp. 584-589.

[5] P. F. Fischer, "Algorithm and implementation uncertainty in viewshed analysis," Int. Journ. Geog. Inform. Science, 7:4, 331-347, 1993.

[6] S.S. Streeter, D. J. Breton, J. M. Corgan, "Measuring the Non-Line-of-Sight Ultra-High-Frequency Channel in Mountainous Terrain," USACE Engineer Research and Development Center, ERDC/CRREL TR-18-3, March 2018.

[7] G. A. Hufford, A. G. Longley, W. A. Kissick, "A Guide to the Use of the ITS Irregular Terrain Model in the Area Prediction Mode," Ch. 6, pp. 28-37, April 1982.

[8] P.L. Rice, A.G. Longley, K.A. Norton, and A.P. Barsis, "Transmission Loss Predictions for Tropospheric Communication Circuits," U.S. Department of Commerce, Natl. Bur. of Stand., TN 101, Vols. I & II, (Revised January 1, 1967).

[9] Table Mountain Field Site, https://www.its.bldrdoc.gov/resources/table-mountain/tm-home.aspx, accessed Feb. 13, 2019.

[10] C. A. Hammerschmidt, R. T. Johnk, "Understanding the Impact of Terrain Databases on the Irregular Terrain Model," Proc. 2017 IEEE Intl. Symp. EMC/SIPI, Washington, D.C. August, 2017.

[11] Y. Okumura, E. Ohmori, T. Kawano, and K. Fukuda, "Field strength and its variability in VHF and UHF land-mobile radio service," Rev. Elec. Commun. Lab., 16, 9-10, pp. 825-873, Sept.-Oct. 1968.

[12] M. Hata, "Empirical formula for propagation loss in land mobile radio services," IEEE Transactions on Vehicular Technology, VT-29, 3, pp. 317-325, Aug. 1980.

[13] C. A. Hammerschmidt, R. T. Johnk, "Extracting Clutter Metrics From Mobile Propagation Measurements in the 1755-1780 MHz Band," Proc. 2016 IEEE Military Comm. Conf., Baltimore, MD, November, 2016.

[14] LandFire, https://www.landfire.gov/, accessed 3/3/2019.

[15] ESRI-ArcGIS, https://www.esri.com/en-us/about/about-esri/overview, accessed 3/3/2019.

[16] QGIS, https://docs.qgis.org/2.18/en/docs/index.html, accessed 3/3/2019.

[17] E. Drocella, J. Richards, R. Sole, F. Najmy, A. Lundy, P. McKenna, "3.5 GHz Exclusion Zone Analyses and Methodology," Natl. Telecomm. Infor. Admin., NTIA-TR-15-517, Appendix A, (Reissued March 2016).

[18] USGS, National Land-Cover Database, https://www2.usgs.gov/climate_landuse/lcs/projects/nlcd.asp, accessed 3/8/2019.

[19] Department of Commerce Boulder Laboratories, http://www.boulder.doc.gov/, accessed 3/3/2019.

[20] C. A. Hammerschmidt, "ISART Conference 2015, https://www.its.bldrdoc.gov/media/66183/hammerschmidt_johnk.pdf, accessed 3/3/2019.

This paper was presented at, and appears in the proceedings of, the 2019 IEEE International Symposium on Electromagnetic Compatibility, Signal & Power Integrity (EMC+SIPI). IEEE